

DEEP CHANDRA & HUBBLE OBSERVATIONS OF NGC 4697, THE NEAREST OPTICALLY LUMINOUS, X-RAY FAINT ELLIPTICAL GALAXY

Gregory R. Sivakoff

Advisor: Craig L. Sarazin

Department of Astronomy, University of Virginia

Abstract

With NASA's *Chandra X-ray Observatory*, we have accumulated over two days of data from NGC 4697, the nearest optically luminous, X-ray faint elliptical galaxy. These observations provide one of the deepest views of low-mass X-ray binaries (LMXBs; binary stars, with one normal star with $M \lesssim M_{\text{Sun}}$ and either a neutron star or black hole, which emit profuse amounts of X-rays) in an elliptical galaxy. In addition to detecting lower luminosity LMXBs, these observations allow us to probe the variability behavior of the brighter LMXBs. We discover flaring behavior with no clear analog in our own Galaxy and derive the timescales over which LMXBs may be transient. With our *Hubble Space Telescope* observations, which reveal the population of globular clusters (GCs; dense, spherical concentrations of millions of stars), we find that approximately one-third of the LMXBs are in GCs and that approximately one-tenth of the GCs contain LMXBs. We explore various aspects of the LMXB-GC connection. These explorations, when combined with data from other galaxies, will allow us to answer questions about the formation and evolution of LMXBs, GCs, and elliptical galaxies.

Introduction

In a typical elliptical galaxy (classified optically by its ellipsoidal shape, in contrast to spiral galaxies whose shapes are dominated by a flattened disk with spiral structure) no star formation has occurred for billions of years. Since the most massive stars (stars with $M \gtrsim 8M_{\text{Sun}}$) burn their nuclear fuel quickly ($t \lesssim 3 \times 10^7$ yr), the only remnants of massive stars in elliptical galaxies are stellar-mass black holes (BHs) and neutron stars (NSs). These objects, the end-states of massive stars, have such strong gravity that they are two of the most extreme types of objects in the Universe. By themselves, BHs/NSs are not detectable in nearby elliptical galaxies. If there is a normal star closely orbiting the BH/NS (i.e., a close binary star), the gravity from the BH/NS can pull off the outer envelope of the normal star. As the material from the stellar envelope accretes onto the BH/NS, the material reaches millions of degrees, and emits X-rays. Since there are no massive stars in elliptical galaxies, these systems must be low-mass X-ray binaries (LMXBs; so named because the normal star has $M \lesssim M_{\text{Sun}}$).

Elliptical galaxies are luminous X-ray sources (Forman, Jones, & Tucker 1985). For galaxies of a given optical luminosity, the X-ray-to-optical luminosity ratio (L_X/L_B) ranges over two orders of magnitude (Canizares, Fabbiano, & Trinchieri 1987; White & Davis 1997). We refer to galaxies with relatively high L_X/L_B ratios as “X-ray bright” and to galaxies with relatively low L_X/L_B ratios as “X-ray faint.” Hot ($kT \sim 1$ keV) gas located between the stars dominates the X-ray emission in X-ray bright galaxies (e.g., Forman et al. 1985; Trinchieri, Fabbiano, & Canizares 1986); whereas X-ray faint galaxies exhibit two distinct spectral components: a hard (~ 1 – 2 keV) component (Matsumoto et al. 1997) and a very soft (~ 0.2 keV) component (Fabbiano, Kim, & Trinchieri 1994; Pellegrini 1994; Kim et al. 1996). Since the hard component is actually found in both X-ray bright and X-ray faint early-type galaxies, with strengths roughly proportional to the optical luminosity of the galaxy, Kim et al. (1992) suggested that the hard component is due to LMXBs like those observed in the Milky Way's bulge.

The *Chandra X-ray Observatory*¹ is one of NASA's Great Observatories. Launched 1999 July 23, this satellite uses four nested pairs of grazing incidence (small angle reflection) paraboloid and hyperboloid mirrors to collect and classify individual X-ray photons with energies of 0.1–13 keV. Its ability to see details on $\sim 0''.5$ (the equivalent of being able to see the two headlights on a car from about 400 miles away) and its relatively large collecting area (400 cm^2 at 1 keV) make it ideal for studying individual LMXBs in nearby elliptical galaxies. A single chip of the Advanced CCD Imaging Spectrometer (ACIS) has a $\sim 8' \times 8'$ field-of-view (FOV); most nearby elliptical galaxies fit on a single chip. The large sample of bright LMXBs ($L_X > 10^{37} \text{ erg/s}$) in elliptical galaxies (~ 50 – 200 per galaxy, e.g., Sarazin et al. 2000, 2001; Angelini et al. 2001; Sivakoff et al. 2003) allows studies of LMXB formation and evolution that complement what we can do in our own Galaxy with its ~ 150 active LMXBs ($L_X > 10^{36} \text{ erg/s}$).

The *Hubble Space Telescope*² (*HST*) is also one of NASA's Great Observatories. It was launched 1990 April 24, and has been upgraded by four service missions. Typical reflecting mirrors (a concave primary plus a con-

¹ See <http://chandra.harvard.edu>

² See <http://hubblesite.org>

vex secondary) collect the intensity of light with wavelengths (λ from 200–2400nm) depending on the instrument used. Since *HST* orbits above the atmosphere, its ability to see detail (called resolution) is diffraction limited; since the primary mirror is 2.4m, its resolution at 1000nm is $\sim 0.''1$ (the equivalent of being able to see the two headlights on a car from about 2000 miles away). At the distance of most of the nearby elliptical galaxies, *HST* can resolve objects with diameters that are $\gtrsim 20$ ltyr. In the last servicing mission, the Advanced Camera for Surveys (ACS) was installed. ACS samples its $\sim 3' \times 3'$ FOV (twice that of the previous imaging instrument) at the best resolution *HST* can achieve.

Globular clusters (GCs) are spherical concentrations of tens of thousands to million of stars (Binney & Tremaine 1987). The stars are so tightly packed that the density of stars can reach 10^7 times the density of stars near the Sun. Typical GCs are ~ 60 ltyr in diameter³. In the Milky Way, $\sim 10\%$ of LMXBs are located in globular clusters; however, GCs account for a much smaller fraction of the optical light in the Galaxy. It has long been recognized that GCs are more efficient at producing LMXBs (by a factor of ~ 300) than the field. This greater efficiency is attributed to dynamical interactions of stars in the dense environments of GCs (e.g., Katz 1975; Clark 1975).

To study the LMXB-GC connection in elliptical galaxies, we need to know the properties of both populations. The existing lists of GCs for elliptical galaxies are rather incomplete. Since atmospheric effects blend the GCs into the diffuse galaxy emission, ground-based observations generally do not detect GCs from the inner regions of elliptical galaxies, where most of their LMXBs are located. Additionally, GCs are not resolved in ground-based optical images of galaxies at the distance of most nearby elliptical galaxies; candidate GCs are identified by luminosities and (potentially) colors. Therefore, many of the candidate GCs may be unrelated faint optical objects. Since *HST* orbits the Earth, there are no atmospheric effects to blend the GCs into the diffuse galaxy emission. *Hubble* can detect GCs in the inner regions of galaxies and measure their shape. Prior to the installment of the ACS, only a small portion of a galaxy could be surveyed in a single observation. Taking advantage of the ACS capabilities, the ACS Virgo Cluster Survey & ACS Fornax Cluster Survey are obtaining deep, high-resolution F475W and F850LP images of the central $\sim 3' \times 3'$ of 144 nearby elliptical galaxies. One of their products is a sample of extragalactic GCs with unprecedented depth and uniformity. From these *HST* ACS images, thousands of GCs associated with these galaxies will be identified and their positions, magnitudes, colors,

³*HST* can resolve GCs in nearby elliptical galaxies.

metallicities (abundance of elements besides hydrogen and helium) and structural parameters will be derived. We are working with the PIs of both surveys to compare the LMXBs and GCs in elliptical galaxies.

The (Pre-ACS) connection between GCs and LMXBs is stronger in elliptical galaxies than the Milky Way, with ~ 20 – 70% of the LMXBs being associated with GCs (Sarazin et al. 2000, 2001; Angelini et al. 2001; Kundu et al. 2002). It has been suggested that most of the LMXBs in elliptical galaxies were made in GCs (Grindlay 1984; Sarazin et al. 2001; White et al. 2002), with the LMXBs outside of GCs (field LMXBs) ejected from GCs by kicks from the explosive deaths of dying stars, stellar dynamical interactions, or the dissolution of the GC due to tidal effects. If so, then the LMXBs (field + GC) would be a direct probe of their initial GC populations and GC destruction processes. On the other hand, it has been recently claimed that the relationship between the fraction of LMXBs formed in GCs and the GC specific frequency (the number of GCs per unit optical luminosity) in elliptical galaxies is more consistent with the field LMXBs being formed in the field (Juett 2005).

NGC 4697 is the nearest ($\sim 4 \times 10^7$ ltyr; Tonry et al. 2001) optically luminous ($M_V < -20$), X-ray faint elliptical galaxy. Since it is so close, X-ray observations allow study of fainter LMXBs than more distant elliptical galaxies. Based on its high optical luminosity, we expect a large number of LMXBs. Since it is X-ray faint, there is only a small contribution to the X-ray emission by diffuse gas, making it easier to detect the LMXBs. Sarazin et al. (2000, 2001) used *Chandra* to resolve the X-ray emission into ~ 90 LMXBs. We have reobserved NGC 4697 with *Chandra* to study fainter LMXBs that were unresolved in the earlier observation and study the variability of LMXBs. We also have obtained *HST* observations of NGC 4697 to study the GCs and the LMXB-GC connection.

Chandra Observations & Analysis

Chandra has observed NGC 4697 five times (observations 0784, 4727, 4728, 4729, and 4730), 2000 January 15, 2003 December 26, 2004 January 06, February 02, and August 18 using ACIS. We determined the pointing of the observations so that the entire galaxy was located on the S3 chip. Therefore, the analysis of NGC 4697 in this paper will be based on data from the S3 chip alone; a number of serendipitous sources seen on the other chips are unlikely to be related to NGC 4697.

For each individual observation, we detected sources using the wavelet detection algorithm (CIAO WAVDETECT program) in the 0.3–6keV energy band, detecting 97, 78, 87, 77, and 98 sources. The coordinates of ~ 50 matching sources between observations were used

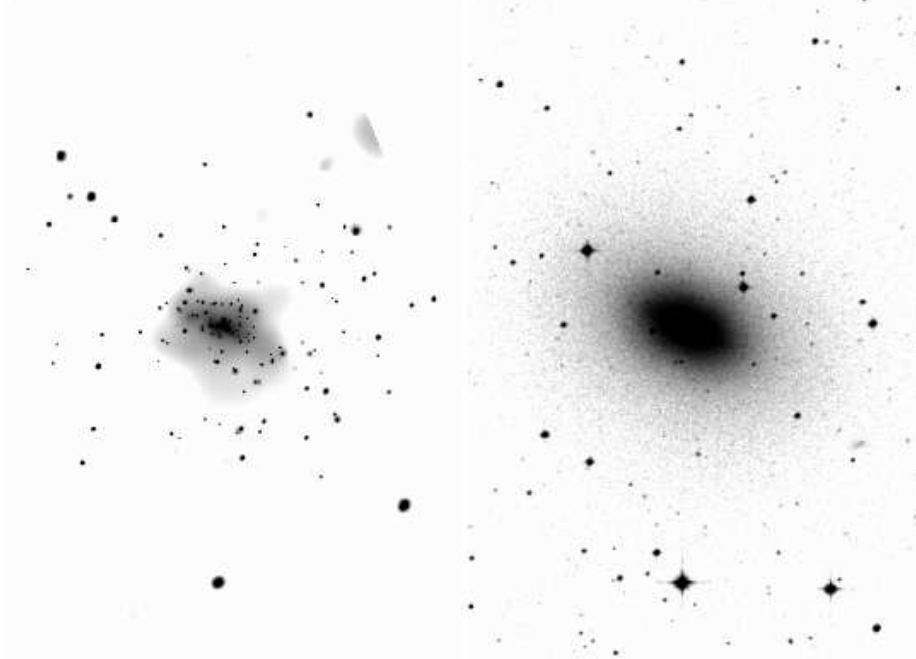


Fig. 1.— (Left) Adaptively smoothed *Chandra* X-ray image of the LMXBs and diffuse hot interstellar gas in NGC 4697 ($\sim 600'' \times 900''$). (Right) Digitized Sky Survey Two Red optical image of the same region.

to align the astrometry. A combined 185 ks image was created (See Figure 1). From this image, we detected 158 sources that dominate the X-ray emission. There is some diffuse emission remaining that is a combination of currently undetectable point sources and diffuse gas emission. We refined the source positions and created source extraction regions for the 90% encircled energy using ACIS Extract 3.34 (Broos et al. 2002). Based on 7 well matched sources, we estimate our absolute astrometry is accurate to $0.4''$, except near the edges of the chip where the PSF is large. Aperture photometry was performed separately on each observation and then combined for all analysis. Of the 158 detected sources, 126 have their flux determined at the 3σ level and 121 have more than 20 net counts.

We determined the combined spectra of all significantly detected sources that lie within the elliptical region of constant surface brightness that contains half of the optical light. With this spectrum (power-law, $N(E) \propto E^{-\Gamma}$ where $\Gamma = 1.47$, and Galactic absorption) and the distance of NGC 4697, we can convert the observed count rates of the sources into luminosities. This conversion is vital because a contaminant is settling on the satellite's optical filter and decreasing the instrument's sensitivity with time.

The five observations of NGC 4697 provide for a detailed look at the variability of LMXBs in elliptical galaxies. Galactic X-ray binaries (XRBs) exhibit a wide-

range of timescale variability ($<$ milliseconds – years). Due to the frame time of ~ 3 s in our *Chandra* data, the shortest timescale flaring we could detect is on the order of seconds. A bright LMXB (10^{38} erg s^{-1}) will have only ~ 25 counts in a ~ 40 ks *Chandra* observation of NGC 4697. We have developed a new statistical technique for detecting short-timescale flare behavior among such low source counts (Sivakoff et al. 2005). This technique can be applied to a single observation, but with multiple observations, weaker flares can be significantly detected if the flaring occurs multiple times. Figure 2 displays a source with short-timescale flare behavior that was significantly detected in a single observation. Its flare luminosity ($\sim 6 \times 10^{39}$ erg s^{-1}) is above a theoretical steady-state limit for a NS and is similar to the peak luminosities of the brightest Galactic BH-XRBs. However, the flare duration (~ 70 s) is much shorter than are typically seen for outbursts reaching those luminosities in Galactic BH sources. Other weaker flares were seen, with luminosities approximately a factor of ten weaker, but durations more than a factor of ten larger. Although the luminosity and outburst duration of these other sources are similar to a known flaring behavior (Type I X-ray Superbursts), they recur on much shorter timescales (days as opposed to years). The flare behavior in the first source, and perhaps the two other sources displaying weaker flares, have no clear Galactic analog. We may be observing a new phenomena in X-ray binaries.

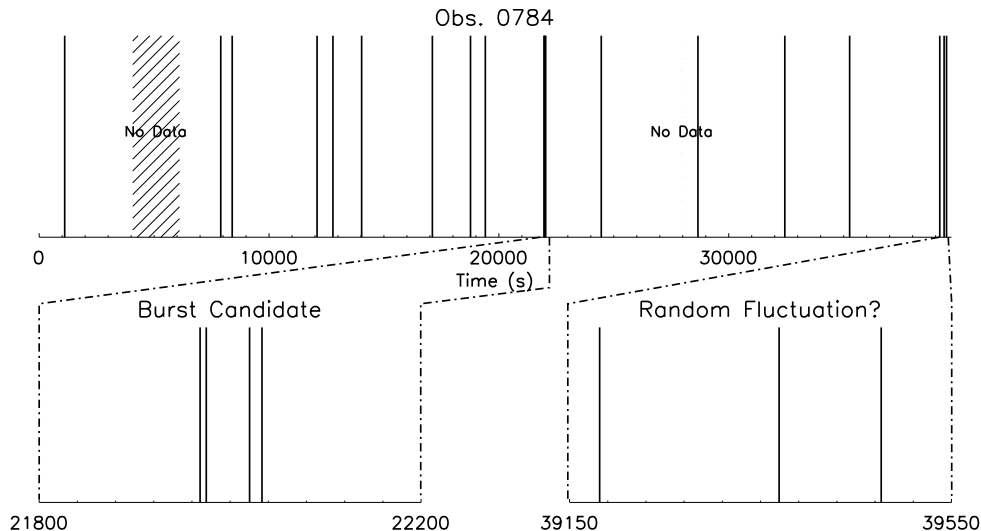


Fig. 2.— Vertical lines represent times a photon arrived from CXOU J124839.0–054750. Twenty photons arrived in ~ 40 ks; however, four of those photons (the burst candidate photons) arrive in ~ 70 s. Statistical techniques are used to infer that this flare is unlikely to be a random statistical fluctuation. On the other hand, the three photons that fall in ~ 300 s can not be distinguished from a random fluctuation.

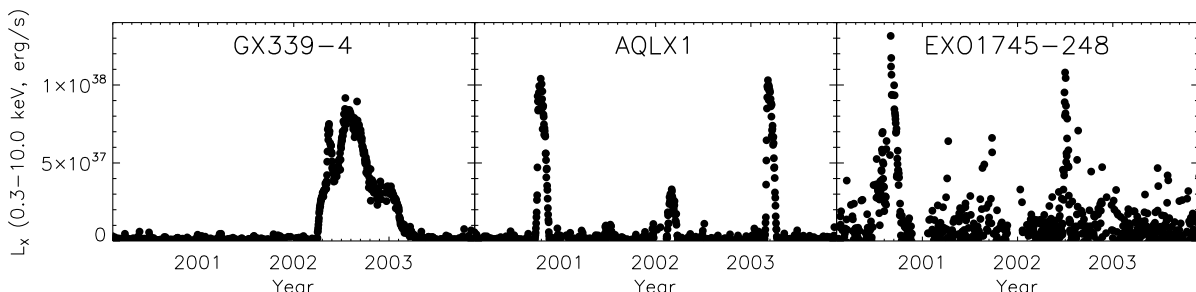


Fig. 3.— Rough luminosities of transient Galactic sources (converted Rossi X-ray Timing Explorer All Sky Monitor counts assuming unabsorbed power-law spectra of $\Gamma=2$). Left–right: a BH-LMXB, field-NS-LMXB, and GC-NS-LMXB.

In our own Galaxy, longer time-scale variations, such as transient sources are also observed (Figure 3). To calculate the lifetime of a source, one needs to know its fuel reservoir and the rate at which it burns its fuel. As Figure 3 shows, the rate can vary dramatically. These transient outbursts can occur ~ 1 per year or once in the history of X-ray astronomy. It is therefore important to understand the behavior of transient and variable sources. Most of the sources in NGC 4697 do not show the level of transience as seen in Figure 3. Instead they seem to be longer persistent sources. There are nine sources (e.g., Figure 4) that do show transient behavior. If the sources observed to be persistently bright are actually transient sources with long outburst durations, and all sources have the same average duration, then we calculate the average duration is ~ 130 yr. Assuming a recurrence

timescale of ~ 1500 year (Rutledge et al. 2002), the duty cycle (the ratio of time spent actively emitting to time between outbursts, $\sim 9\%$) suggests that lifetimes calculated based on the active luminosity are ~ 11 times too small and that there are ~ 11 times as many quiescent LMXBs ($L \lesssim 10^{33} \text{erg s}^{-1}$) as active LMXBs ($L \gtrsim 10^{37} \text{erg s}^{-1}$). The latter is comparable to the one active LMXB and seven quiescent LMXBs found recently in a Galactic GC by Heinke et al. (2003). The lifetimes and total numbers of LMXBs are important constraints for theories of LMXB evolution.

Hubble Observations & Analysis

We observed the center of NGC 4697 with *Hubble Space Telescope Advance Camera for Surveys* (HST-ACS), acquiring two 375s exposures in the F475W

(g_{475}) band, two 560s exposures in the F850LP (z_{850}) band, and one 90s F850LP exposure (e.g., Figure 5). Source detection and characterization were performed as in Jordán et al. (2004a), with small adjustments made for the relative proximity of NGC 4697. SExtractor (Bertin & Arnouts 1996) was used to detect sources of $S/N = 10$. A triangle-based search algorithm was then used to align the detected sources between exposures. A multidrizzle technique (Koekemoer et al. 2002) was used to transform the detector coordinates to sky coordinates, as well as reject cosmic rays. After weight-images were created to evaluate the sensitivity in each pixel and the elliptical profile of the stellar light in the galaxy was removed, SExtractor was used to detect the remaining GCs and other optical sources with a detection threshold of 5 connected pixels at a 1.5σ significance level. For NGC 4697, 703 optical sources were detected. The photometric and structural parameters of those sources were measured by fitting the two-dimensional ACS surface brightness profiles with PSF-convolved isotropic, single-mass King (1966) models. Approximately 300 globular clusters were identified by their colors ($0.5 \leq g_{475}z_{850} \leq 1.6$) and their shapes (half the GC light must be within $\gtrsim 3$ ltyr). The luminosity function (Figure 6) of the GCs are roughly consistent with the typical Galactic GC model (turnover at $M_V = -7.4$, assuming $v - z \sim 0.8$). The color distribution (Figure 7) shows a clearly bimodal population of blue GCs ($g_{475} - z_{850} \sim 0.9$) and red GCs ($g_{475} - z_{850} \sim 1.2$). These two populations probably represent two different bursts of star-formation. The red

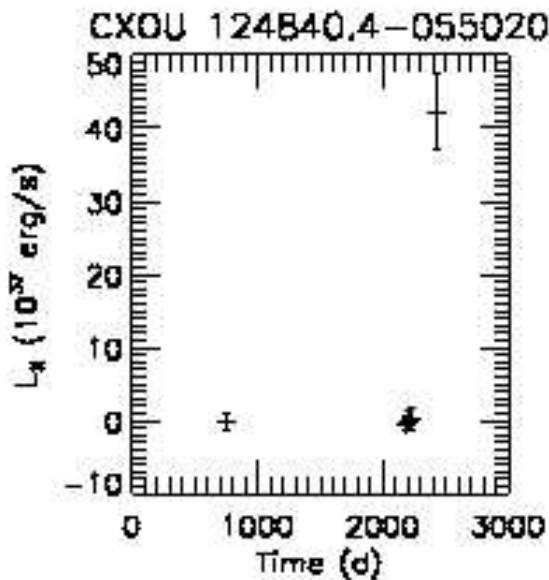


Fig. 4.— Luminosity as a function of time since observation 0784 for one of the transient sources in NGC 4697.

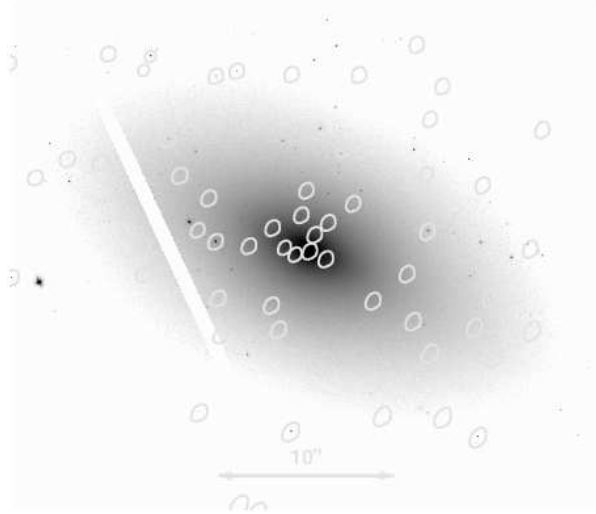


Fig. 5.— HST image(z_{850} , $\sim 30'' \times 30''$). The white polygons are the 90% encircled energy regions of LMXBs detected by Chandra. Of the LMXBs, $\sim 36\%$ are coincident with a GC.

GCs are probably more metal-rich than the blue GCs; however, the standard age-metallicity uncertainty means the blue GCs could just be younger than the red GCs.

LMXB-GC Connection

We have identified 299 GCs; there are 89 X-ray sources in the ACS FOV. X-ray sources within $1''$ of a globular cluster source were considered matched; the probability of a random GC matching an LMXB is $\sim 4\%$. If there were no LMXB-GC connection, then we would expect ~ 4 matches; we find 34 matches. Since there is an LMXB-GC connection, we have found a self-consistent solution with 32/89 LMXBs being physically associated with a GC, 2/89 LMXBs begin randomly associated with a GC, and 55/89 field LMXBs. Approximately 36% of the LMXBs are in GCs, consistent with results from other galaxies. Approximately 10% of the GCs contain a bright LMXB ($L \gtrsim 10^{37} \text{ erg s}^{-1}$). This number is about 2.5 times what is typically seen; however, the NGC 4697 observations are able to detect fainter LMXBs. We note that in the Milky Way, 10% of the GCs contain an active LMXB ($L \gtrsim 10^{36} \text{ erg s}^{-1}$).

In Figures 6 and 7, we also display the histograms of the GCs containing a bright LMXB. From both figures it is clear that the GCs containing bright LMXBs do not have the same properties of the other GCs. Kolmogoroff-Smirnov tests show that there is a 0.05%, 0.03%, and 0.04%, that the LMXB-GCs are drawn from the same population of g_{475} magnitudes, z_{850} magnitudes, and $g_{475} - z_{850}$ colors. Similarly, Wilcoxon rank-sum tests show these results are 4.0σ , 4.6σ , and 2.8σ significant.

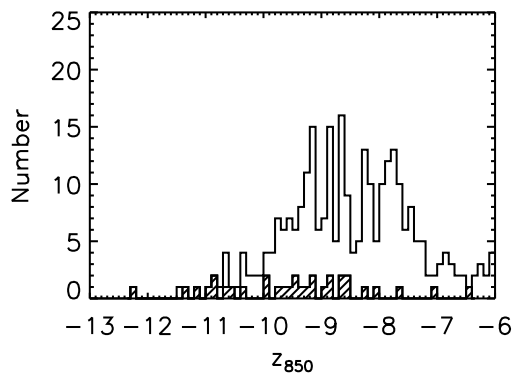


Fig. 6.— Luminosity histogram (z_{850}) of the GCs in NGC 4697. The hashed histogram indicates the GCs that contain LMXBs. Under the astronomical magnitude system, brighter objects are smaller. Brighter GCs tend to have LMXBs.

Brighter GCs and redder GCs are more likely to contain an LMXB. The first result, brighter GCs are more likely to contain an LMXB, is most likely due to brighter GCs having more stars, and thus a higher probability of forming an active LMXB than fainter GCs. The second result, redder GCs are more likely to contain an LMXB, is probably due to a deeper astrophysical relation. Typically, redder GCs are interpreted as being more metal-rich than bluer GCs. There are three possible mechanisms discussed in the literature in which higher metallicity GCs may have a higher chance of having LMXBs. First, metal-rich stars may have larger radii and masses compared to metal-poor stars (Bellazzini et al. 1995). This would make it easier to form LMXBs. Second, metal-rich stars may produce more NSs/BHs per unit mass; for instance, the initial number of stars as a function of mass (IMF) could vary (Grindlay 1987). A larger number of NSs/BHs would increase the number of LMXBs that can form. Finally, irradiation-induced winds, which would be weaker in metal-rich stars due to more efficient metal line cooling, slow down the evolution of LMXBs in metal-rich clusters (Maccarone et al. 2004). With a longer lifetime, more LMXBs would be observed at any given time since their formation in the more metal-rich clusters. Jordán et al. (2004b) used Deep *Chandra/HST* observations of LMXBs in M87, the central elliptical galaxy in the Virgo cluster, to find that the first mechanism is unlikely to provide the necessary enhancement.

Future Work

The analysis of the data provided by combined observations of elliptical galaxies using *Chandra* and *HST* is ongoing. With deep observations of NGC 4697, M87

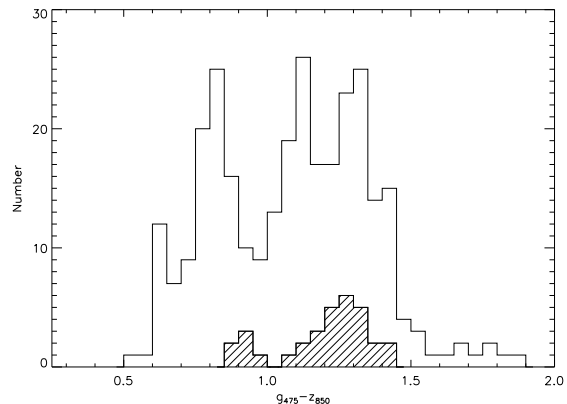


Fig. 7.— Color histogram ($g_{475} - z_{850}$) of the GCs in NGC 4697. The hashed histogram indicates the GCs that contain LMXBs. Under the astronomical magnitude system, redder objects are larger. Redder GCs are approximately three times as likely to contain LMXBs.

(Jordán et al. 2004b), and new data that we are acquiring this year for NGC 4365, another elliptical galaxy, we will provide the templates with which we will interpret data from a larger sample. Between the *HST*-ACS Virgo Cluster Survey and the the *HST*-ACS Fornax Cluster Survey, the centers of 144 elliptical galaxies will be observed optically. Of these galaxies, 39 have existing, scheduled, or proposed *Chandra* observations. We will use the large sample of LMXBs from these galaxies to gain insight into the formation and evolution of LMXBs, GCs, and elliptical galaxies. In particular, we will compare the spatial distributions of LMXBs, GCs, and stellar light from galaxies to determine the origin of field LMXBs and simultaneously test models for the destruction of GCs. We will also test models that predict which GCs will be likely to contain an LMXB in an effort to constrain the formation and evolution of GCs. Where available, we will use the spectroscopically determined ages of GCs to compare star formation histories of entire galaxies to the star formation history tracked by LMXBs. In data-sets with multiple observations, we will use the variability properties of LMXBs to explore possible new flare behavior, and to constrain the evolution of LMXBs.

References

- Angelini, L., Loewenstein, M., & Mushotzky, R. F. 2001, *ApJ*, 557, L35
- Bellazzini, M., Pasquali, A., Federici, L., Ferraro, F. R., & Pecci, F. F. 1995, *ApJ*, 439, 687
- Bertin, E., & Arnouts, S. 1996, *A&AS*, 117, 393

- Binney, J., & Tremaine, S. 1987, *Galactic dynamics* (Princeton, NJ, Princeton University Press)
- Broos, P., Townsley, L., Getman, K., & Bauer, F. 2002, ACIS Extract, An ACIS Point Source Extraction Package, Pennsylvania State University
- Canizares, C. R., Fabbiano, G., & Trinchieri, G. 1987, *ApJ*, 312, 503
- Clark, G. W. 1975, *ApJ*, 199, L143
- Fabbiano, G., Kim, D.-W., & Trinchieri, G. 1994, *ApJ*, 429, 94
- Forman, W., Jones, C., & Tucker, W. 1985, *ApJ*, 293, 102
- Grindlay, J. E. 1984, *Advances in Space Research*, 3, 19
- Grindlay, J. E. 1987, in *IAU Symp. 125: The Origin and Evolution of Neutron Stars*, 173
- Heinke, C. O., Grindlay, J. E., Lugger, P. M., Cohn, H. N., Edmonds, P. D., Lloyd, D. A., & Cool, A. M. 2003, *ApJ*, 598, 501
- Jordán, A., et al. 2004a, *ApJS*, 154, 509
- . 2004b, *ApJ*, 613, 279
- Juett, A. M. 2005, *ApJ*, 621, L25
- Katz, J. I. 1975, *Nature*, 253, 698
- Kim, D.-W., Fabbiano, G., Matsumoto, H., Koyama, K., & Trinchieri, G. 1996, *ApJ*, 468, 175
- Kim, D.-W., Fabbiano, G., & Trinchieri, G. 1992, *ApJ*, 393, 134
- King, I. R. 1966, *AJ*, 71, 64
- Koekemoer, A. M., Fruchter, A. S., Hook, R. N., & Hack, W. 2002, in *The 2002 HST Calibration Workshop*, ed. S. Arribas, A. Koekemoer, & B. Whitmore (Baltimore, MD: Space Telescope Science Institute), 339
- Kundu, A., Maccarone, T. J., & Zepf, S. E. 2002, *ApJ*, 574, L5
- Maccarone, T. J., Kundu, A., & Zepf, S. E. 2004, *ApJ*, 606, 430
- Matsumoto, H., Koyama, K., Awaki, H., Tsuru, T., Loewenstein, M., & Matsushita, K. 1997, *ApJ*, 482, 133
- Pellegrini, S. 1994, *A&A*, 292, 395
- Rutledge, R. E., Bildsten, L., Brown, E. F., Pavlov, G. G., Zavlin, V. E., & Ushomirsky, G. 2002, *ApJ*, 580, 413
- Sarazin, C. L., Irwin, J. A., & Bregman, J. N. 2000, *ApJ*, 544, L101
- . 2001, *ApJ*, 556, 533
- Sivakoff, G. R., Sarazin, C. L., & Irwin, J. A. 2003, *ApJ*, 599, 218
- Sivakoff, G. R., Sarazin, C. L., & Jordán, A. 2005, *ApJ*, in press
- Tonry, J. L., Dressler, A., Blakeslee, J. P., Ajhar, E. A., Fletcher, A. B., Luppino, G. A., Metzger, M. R., & Moore, C. B. 2001, *ApJ*, 546, 681
- Trinchieri, G., Fabbiano, G., & Canizares, C. R. 1986, *ApJ*, 310, 637
- White, R. E., & Davis, D. S. 1997, in *ASP Conf. Ser. 115, Galactic Cluster Cooling Flows*, ed. N. Soker (San Francisco: ASP), 217
- White, R. E., Sarazin, C. L., & Kulkarni, S. R. 2002, *ApJ*, 571, L23